HHS Public Access

Author manuscript

Addict Biol. Author manuscript; available in PMC 2019 June 12.

Published in final edited form as:

Addict Biol. 2018 March ; 23(2): 824–835. doi:10.1111/adb.12532.

Aberrant blood-oxygen-level-dependent signal oscillations across frequency bands characterize the alcoholic brain

Jui-Yang Hong[1], **Eva M. Müller-Oehring**[1,2], **Adolf Pfefferbaum**[1,2], **Edith V. Sullivan**[2], **Dongjin Kwon**[1], and **Tilman Schulte**[1,3]

[1]Neuroscience Program, Center for Health Sciences, SRI International, Menlo Park, CA USA

[2]Department of Psychiatry & Behavioral Sciences, Stanford University, Stanford, CA USA

[3]Pacific Graduate School of Psychology, Palo Alto, CA USA

Abstract

Chronic alcoholism is associated with widespread regional differences from controls in brain activity and connectivity dynamics measured by blood-oxygen-level-dependent (BOLD) signals. Identification of alcoholism-related neurofunctional power dynamics using functional magnetic resonance imaging (fMRI) that relate to cognition and behavior may serve as biomarkers of alcoholism. Previously, resting-state fMRI studies examined BOLD signals at a single low-frequency (LF) bandwidth. BOLD signals, however, oscillate systematically at different frequencies and are organized in a resting brain where LF oscillation facilitates long-distance communication between regions across cortical regions, whereas high-frequency (HF) oscillation occurs in closely localized, subcortical areas. Using a frequency power quantification approach, we investigated whether the organization of BOLD signal oscillations across all measured frequency bandwidths is altered in alcoholism and relates to cognitive performance. Frequency-dependent oscillation power differences between 56 sober alcoholics and 56 healthy controls occurred for all frequency bands. Alcoholics exhibited greater frequency oscillation power in the orbitofrontal cortex and less power in the posterior insula within the HF bandwidth than controls. Aberrant orbitofrontal HF power was associated with poorer memory performance and slower psychomotor speed in alcoholics. Middle-frequency and LF power proved sensitive in detecting altered frequency oscillation dynamics in parietal and postcentral cortical regions of alcoholics. This study is novel in identifying alcohol-related differences in BOLD oscillation power of the full fMRI frequency bandwidth. Specifically, HF power aberrations were associated with poorer cognitive functioning in alcoholism and may serve as a biomarker for identifying neural targets for repair.

Keywords

alcoholics; BOLD oscillation; fMRI

Correspondence to: Tilman Schulte, Center for Health Sciences, SRI International, 333 Ravenswood Ave, Menlo Park, CA 94025, USA. tilman.schulte@sri.com.

Authors Contribution JYH and EMOe designed and performed the research. AP, EVS and TS contributed analytic tools. JYH, AP, DK and EMOe analyzed the data. JYH, EMOe, EVS and TS wrote the paper.

INTRODUCTION

Chronic excessive alcohol consumption is known to affect neurophysiological and cognitive functions that contribute to self-awareness, attention, memory, reward and control over addictive behavior (Loeber *et al.* 2009; Müller-Oehring & Schulte 2014). These abilities are linked to specific functional brain systems including the executive control, salience, attention and reward networks (Camchong, Stenger, & Fein 2013; Courtney, Ghahremani, & Ray 2013; Weiland *et al.* 2013). Neural networks have been identified with functional connectivity methods measuring synchrony of spontaneous blood-oxygen-level-dependent (BOLD) fluctuations (Biswal *et al.* 1995). Typically, regional activation and functional connectivity analyses focus on a single low-frequency (LF) oscillation band, usually between 0.01 and 0.1 Hz, which are sensitive to BOLD fluctuation in cortical regions but exclude information from high-frequency (HF) bandwidths that are sensitive to BOLD fluctuation in subcortical regions (Malinen *et al.* 2010; Baria *et al.* 2011). To date, the effect of chronic alcoholism on BOLD-derived neurofunctional power dynamics across the whole frequency bandwidth has not been studied, and how the multi-band frequency power data relate to cognitive and motor abilities is unknown. Knowledge of these relations could lead to a mechanistic understanding of alcoholism-related impairment.

Information on alcohol-related regional brain disruption or sparing of other frequency bandwidths of the BOLD signal can be gained by employing the amplitude of low frequency fluctuation (ALFF) approach for analyzing resting-state functional magnetic resonance imaging (fMRI) data. ALFF measures the power spectrum intensity of intrinsically spontaneous BOLD frequency fluctuation (Zang *et al.* 2007), enabling quantification of the oscillatory BOLD signal along a broad range of frequencies and optimizing detection of localized dynamics of BOLD oscillation properties. Systematic frequency power distributions underlie the structural and functional organization of the human brain where greater LF frequency power occurs in cortical regions, whereas greater HF frequency power occurs in subcortical regions (Baria *et al.* 2011). In addition, specific power spectra reflect specific synaptic connections and brain states while resting or performing tasks (Baria *et al.* 2013). Altered frequency-specific power spectra have also been implicated in clinical diagnoses, including chronic pain, and depressive disorder (Malinen *et al.* 2010; Baliki, Baria, & Apkarian 2011; Yang *et al.* 2016). Moreover, a study of acute alcohol effects on motor and cognitive control functions in non-alcoholics found lower LF oscillation power in the cerebellum and superior frontal gyrus relative to their sober control condition (Zheng *et al.* 2015).

To date, studies of alcoholism using resting-state or task-activated fMRI analyses have not examined alterations in frequency-specific power of BOLD signal oscillation. For the first time, we used the frequency power analysis approach to examine power dynamics of spontaneous BOLD signals in alcoholic men and women compared with sex-matched and age-matched, lowdrinking controls. With previous frequency analyses (Buzsaki & Draguhn 2004; Esposito *et al.* 2013; Zhang *et al.* 2013), we divided the full frequency range of power spectrum into three sub-frequency bands with neurophysiological meanings: the LF band (0.01–0.027 Hz), the middle-frequency (MF) band (0.027– 0.073 Hz) and the HF band (0.073–0.198 Hz). We hypothesized that cortical regions would show greater LF power,

whereas subcortical and limbic regions would have greater HF power independent of study group. Because frequency oscillation power has been linked to brain activities (Baria *et al.* 2013) and its specific power distribution to certain brain regions (Baria *et al.* 2011), we hypothesized that alcoholism-specific compromises in frequency power dynamics would be observed in HF power for subcortical salience regions and in LF and MF power for frontoparietal cortical cognitive control and reward regions. We further hypothesized that frequency power alterations would implicate cognitive abilities and behavioral performance including episodic memory and psychomotor speed, which are commonly affected in chronic alcoholism (Le Berre & Sullivan 2016).

MATERIALS AND METHODS

Subjects

The dataset comprised 56 alcoholic subjects (17 women) and 56 age-matched healthy controls (17 women) (Table 1). The 56 alcoholics were recruited from local rehabilitation or addiction treatment centers through advertisements, referral or word of mouth. The controls were volunteers from the local communities. All the subjects provided written informed consent to participate in this study. The recruitment and study procedures were approved by the Institutional Review Boards of Stanford University School of Medicine and SRI International.

Screening was conducted by clinical research psychologists or research nurses on the basis of the Structured Clinical Interview for DSM-IV (First *et al.* 2012). For all subjects, the exclusion factors were DSMIV criteria for other Axis I diagnoses. In the alcoholic group, 55 subjects met DSM-IV criteria for alcohol dependence, and one subject met criteria for alcohol abuse. Of those meeting dependence criteria, 35 were in early full remission (met no alcohol dependence criteria for <1 year), 12 were in sustained full remission (met no alcohol dependence criteria for >1 year), 5 were in early partial remission (met <3 alcohol dependence criteria within the past 12 months) and 4 did not meet remission criteria. The median number of weeks since alcoholics last met dependence criteria was 21.6 weeks [mean = 78.5 weeks, standard deviation (Padula *et al.*, 2015) = 146.9 weeks]. The median age of alcoholism onset was 25 years [mean = 28.3, standard deviation (SD) = 12.6]. Fifty-five percent of alcoholics and 0 percent of controls met DSM-IV criteria for any type of drug dependence or abuse. The most common type of drug dependence or abuse among alcoholics was cocaine (endorsed by 38 percent of alcoholics), and the median number of weeks since last meeting drug dependence criteria was 406 weeks (mean = 646 weeks, SD = 557 weeks). Significantly more alcoholics met DSM-IV criteria for nicotine dependence (n = 41) than controls (n = 6), $\chi^2(1) = 43.33$, $P < 0.001$ (Fisher's exact test).

Questionnaires, neuropsychological tests and clinical assessments were given before or after scanning and included socioeconomic status, alcohol use disorders identification test (AUDIT) (Babor *et al.* 2001), Beck Depression Inventory (BDI-II) (Beck, Steer, & Brown 1996), Wechsler Test of Adult Reading (WTAR) (Wechsler 2001), Wechsler Memory Scale-Revised (WMS-R) (Wechsler & Stone 1987), California Verbal Learning Test-II (CVLT-II) (Delis *et al.* 2000) and the Digit Symbol subtest of the Wechsler Adult Intelligence Scale-Revised (WAIS-R) (Wechsler 1981).

Imaging data acquisition

All resting-state data required subjects to have their eyes open while in one of two General Electric (Boston, MA, USA) human MRI systems (3T Signa and MR750) with an eight-channel head coil and the same acquisition parameters. MRI scanner system was modeled as a covariate in a separate group-ALFF analysis. Ear plugs and noise-cancelling headphones were used to help reduce the noise from the scanner. The number of subjects scanned by each scanner is shown in Table 1.

Whole-brain rs-fMRI data were acquired with a T2*weighted gradient echo-planar pulse sequence [2D axial; echo time (TE) = 30 ms; repetition time (TR) = 2200 ms; flip angle = 90°; field of view (FOV) = 240 mm; in-plane resolution = 3.75 mm; matrix = 64 × 64; slice thickness = 5 mm; skip = 0 mm; 36 slices]. A dual-echo fast spin-echo scan was obtained for spatial registration using the following parameters: 2D axial; TE = 17 / 102 ms; TR = 5000 ms; flip angle = 90°; FOV = 240 mm; matrix = 256 × 256; slice thickness = 5 mm; skip = 0 mm; 36 slices. To correct for spatial distortions in the echoplanar images, we acquired a field map with a gradientrecalled echo sequence pair (TE = 3/5 ms; TR = 460 ms, slice thickness = 5 mm; skip = 0 mm; 36 slices).

Image preprocessing

Rs-fMRI data preprocessing was performed using STATISTICAL PARAMETRIC MAPPING 8 (SPM8) software Wellcome Trust Centre for Neuroimaging; London, UK; http://www.fil.ion.ucl.ac.uk/spm/software/spm8/). Images were first converted from DICOM into NIFTI format followed by spatial realignment and unwarping of echoplanar images to correct for geometric distortion and head motion. For further analysis, datasets of the 112 subjects had to have motion less than 1.7-mm translation in x, y and z and not exceed 2° rotation in all three directions. Frame-wise displacement values were calculated for individual scans, the maximum displacement was 1.88 and the largest individual mean displacement value was 0.27. Given the lack of consensus in the literature on motion thresholds for scan exclusion (Power, Schlaggar, & Petersen 2015), we followed previous recommendations (e.g., Power *et al.* 2012). The mean unwarped functional images were co-registered with the fast spin-echo anatomical images for each subject. The unwarped functional and anatomical images were then normalized to the standard Montreal Neurological Institute space and resampled to a voxel size of 2 × 2 × 2 mm. A Gaussian kernel of 8-mm full-width at half-maximum was applied to the normalized functional images.

ALFF calculation

Preprocessed functional images were imported into DPARSF 4.0 Advanced toolbox (Data Processing & Analysis of Brain Imaging; http://rfmri.org/dpabi; ChaoGan Yan, New York, NY, USA) (Yan *et al.* 2016) for ALFF calculation. For the frequency power spectrum to be obtained, the time series of each voxel within the individual functional images was transformed into the frequency domain using a fast Fourier transform (Zang *et al.* 2007). The full frequency range was then divided into three frequency bands—LF (0.01–0.027 Hz), MF (0.027–0.073 Hz) and HF (0.073–0.198 Hz)—for further ALFF value calculation (Buzsaki & Draguhn 2004; Esposito *et al.* 2013; Zhang *et al.* 2013). For a given voxel, the absolute

value of the frequency power spectrum was averaged across the predefined frequency band (Zang *et al.* 2007). Note that the scrubbing approach (Power *et al.* 2015), endorsed to correct for outlier frames in resting-state time series analysis, is not recommended for ALFF analysis, because the ALFF calculation is based on fast Fourier transform, which cannot be applied to scrubbed data owing to alteration of its temporal structure by removal of frames (Yan *et al.* 2013). Instead, we used standardized zALFF individuals maps, on the basis of evidence showing reduced motion effects at individual level and increased test–retest reliability with Z-standardization at group analyses (Zuo *et al.* 2010; Yan *et al.* 2013). For Z-standardization, we normalized the ALFF value for each voxel by subtracting the global mean of the ALFF value, and then the value was divided by the SD (Yan *et al.* 2013). In addition, we compared the non-normalized ALFF value of each voxel between alcoholics and controls. There was no significant group difference in the non-normalized ALFF values. Therefore, significant group differences in normalized ALFF comparisons cannot be due to different global means between alcoholics and controls.

ALFF analysis modeling

Individual standardized ALFF maps were implemented in a full-factorial analysis of covariance in SPM8. A secondlevel full-factorial model was used to examine the ALFF differences between the three predefined frequency bands and between alcoholics and controls in each of the three specific frequency bands. Independent groups (controls and alcoholics) and dependent frequency bands (LF, MF and HF) were modeled as factors. The frame-wise displacement values of each individual were calculated by ArtRepair tool (http://cibsr.stanford.edu/tools/human-brain-project/artrepair-software/artrepairinstructions.html) using the six realignment parameters. Alcoholics had on average greater frame-to-frame displacement values than controls (mean displacement: controls 0.088 mm/TR, alcoholics 0.112 mm/TR; SD, controls 0.036, alcoholics 0.05 ; $P = 0.005$). The group difference in frame-wise displacement was small and remained within two voxels shifting. As recommended by Yan *et al.* (2013), Fair *et al.* (2012) and Kong *et al.* (2014) for ALFF group statistics to control for residual motion in the second-level group analysis, we modeled the individual mean frame-wise displacement in addition to individual age, and type of GE scanner as covariates. An explicit gray matter mask created on the basis of the automated anatomical labeling template from MRIcro (http://www.mccauslandcenter.sc.edu/mricro/mricro/template.html) was applied to the model.

Between-frequency ALFF analyses

With previous research showing ALFF value differences across frequency bands (Wang *et al.* 2016), we specified SPM *t*-contrasts between the three predefined frequency bands to examine such differences in ALFF values to reflect the frequency dynamics (HF versus MF, HF versus LF and MF versus LF) in our full-factorial model independent of group differences.

Between-group ALFF analyses

Group-difference contrasts were specified for controls > alcoholics and alcoholics > controls (SPM t-contrast) to examine whether ALFF values for each predefined frequency band were greater or less in the alcoholic group than in the controls.

Statistical significance for ALFF maps

To account for multiple comparisons, frequency and group-difference results were corrected by performing Monte Carlo simulation for two-tailed comparisons as implemented in 3dClustSim (https://afni.nimh.nih.gov/pub/dist/doc/program_help/3dClustSim.html; Robert W. Cox, Bethesda, MD, USA). For this, smoothness parameters of the residual image were calculated using the AFNI program 3dFWHMx (https://afni.nimh.nih.gov/pub/dist/doc/program_help/3dFWHMx.html) and entered into 3dClustSim calculation with 10 000 iterations, and peak threshold probability of 0.005 ($t = 2.81$; two-tailed). A significantly statistical threshold of $P < 0.05$ corrected for multiple comparisons required a contiguous cluster size greater than 131 voxels. This statistical cluster threshold for multiple comparison correction was applied to all second-level *t*-tests.

Statistical analyses of group characteristics

Independent samples *t*-tests were conducted using IBM SPSS v.23 (Armonk, NY, USA) to examine group differences in education, socioeconomic status, lifetime alcohol consumption, days since last drink, AUDIT score, BDI-II score, premorbid IQ (WTAR Standard Score), logical memory (WMS-R total raw score), verbal memory (CVLT-II total free recall score) and graphomotor speed (WAIS-R Digit Symbol) (Table 1). The neuropsychological test scores (premorbid IQ, logical memory, verbal memory and graphomotor speed) were correlated with frequency oscillation power (extracted ALFF values of the regions that showed significant group differences) by using Pearson correlation in IBM SPSS v.23. A statistical significance level was set at $P < 0.05$ after correcting for multiple comparisons using false discovery rate (FDR) (Benjamini, Krieger, & Yekutieli 2006).

RESULTS

ALFF value differences between frequency bands

Independent of diagnosis, differences in frequency power were identified between the three different pairs of frequency bands (LF, MF and HF). Subcortical regions (amygdala, hippocampus, parahippocampus, caudate head, pallidum and insula), anterior temporal lobules, rectus, anterior cingulate cortex, superior frontal cortex (BA8) and cerebellum showed greater oscillation power in the HF than in LF band. By contrast, the posterior cortical (occipital, parietal lobules, angular, supramarginal gyrus, precuneus, posterior cingulate cortex and sensorimotor cortex) and mid-frontal regions (BA46) showed greater frequency fluctuation power in the LF than in HF band (Fig. 1a).

When comparing HF and MF bands, the differences in frequency power distribution patterns (Fig. 1b) were similar to the ones observed between HF and LF bands (Fig. 1a) except for the thalamus. The thalamus showed greater frequency power in the MF band than in the HF band (Fig. 1b).

When comparing MF and LF bands, the frequency power for MF was greater in thalamic and striatal-limbic regions (hippocampus, amygdala, putamen and caudate), the occipital lobe (constrained in calcarine, cuneus and lingual gyrus), posterior insula and anterior

cingulate cortex (Fig. 1c). By contrast, the ALFF values for LF were higher in the cortical regions including the parietal, inferior occipital, inferior temporal, superior frontal (BA6/8), sensorimotor, rectus and orbitofrontal (BA10/11/47) cortices (Fig. 1c).

ALFF value differences between groups

Significant differences in oscillation power between controls and alcoholics were observed in each of the three frequency bands. Within the HF band, the alcoholic group had greater frequency oscillation power in the orbitofrontal cortex (BA10/11/47) and lower power in the posterior insula than the controls (Table 2 and Fig. 2).

Within the MF band, alcoholics had higher ALFF values in the posterior inferior/middle temporal lobules and less oscillation power in the angular and supramarginal gyri than controls (Table 2 and Fig. 3).

Within the LF band, alcoholics showed greater frequency oscillation power in the temporal lobules and postcentral cortex than the controls (Table 2 and Fig. 4), similar to the results observed within the MF band. In addition, alcoholics had lower ALFF values than controls in the supramarginal gyrus and inferior/superior parietal cortex within the LF band (Table 2 and Fig. 4).

Testing whether observed group differences in ALFF power (Table 2) are due to group differences in motion, we correlated residual motion values with regional ALFF power. Mean frame-wise displacement correlated with greater HF orbitofrontal ALFF power, but not differently between groups (controls: $r = 0.29$, $P = 0.03$; alcoholics: $r = 0.27$, $P = 0.046$; $z = 0.11$, $P = 0.91$). There was no significant relationship between motion and ALFF power in any of the other regions in either group. For orbitofrontal HF ALFF power, residual motion accounted for 7 percent of the variance. It did not, however, explain the observed group differences, which remained significant after controlling for motion.

Clinical and behavioral characteristics

Compared with controls, alcoholics had consumed significantly more alcohol ($P < 0.001$), reported more harmful patterns of alcohol usage as measured by the AUDIT ($P < 0.001$), more depressive symptoms (BDI-II) ($P < 0.001$), had lower premorbid IQ as measured by the WTAR ($P < 0.001$), lower logical memory scores for immediate ($P < 0.001$) and delayed recall ($P < 0.001$) as measured by the WMS-R ($P < 0.001$) , lower verbal memory scores for total free recall ($P = 0.002$) and delayed free recall ($P = 0.002$) as measured by the CVLT-II and slower graphomotor speed ($P < 0.001$) reflecting longer time taken to complete the WAIS-R Digit Symbol subtest ($P = 0.001$). Alcoholics also had fewer years of education ($P < 0.001$) and lower socioeconomic status ($P < 0.001$) than controls (Table 1). These comparisons between alcoholics and controls remained significant when using education as a covariate.

ALFF correlation with behavioral tasks and clinical characteristics

In alcoholics, the higher HF orbitofrontal power in alcoholics correlated with poorer logical memory for immediate recall ($r = 0.505$, $P_{unc} = 0.001$, $P_{FDRc} = 0.0007$) and delayed recall

(r = 0.483 , P_{unc} = 0.001, P_{FDRc} = 0.013), poorer verbal memory for total free recall (r = 0.626, P_{unc} < 0.001 , P_{FDRc} = 0.001) and delayed free recall (r = 0.596, P_{unc}-0.001, P_{FDRc} = 0.001), slower graphomotor speed (r = 0.475, P_{unc} = 0.005, P_{FDRc} = 0.047) and longer time to complete the Digit Symbol test (r = 0.537 ,frequency; MF, middle frequency P_{unc} = 0.001, P_{FDRc} = 0.012). In controls, lower HF power of left orbitofrontal cortex was correlated with higher premorbid IQ (left: r = 0.466, P_{unc} = 0.001, P_{FDRc} = 0.008).

DISCUSSION

We systematically evaluated frequency-dependent changes in BOLD signal oscillation power across three physiological frequency bands in alcoholics and controls and identified regionally specific frequency aberrations in alcoholics that were associated with compromised neuropsychological performance, in particular, memory functions. Relatively localized subcortical brain regions had the highest oscillation power within the HF band, while cortical regions exhibited most oscillation power within the LF band. These fundamental frequency power dynamics were present in both alcoholics and controls. Importantly, our full frequency bandwidth examination revealed significant alcoholism-related differences in frequency-dependent power spectrum dynamics that involved the orbitofrontal cortex, parietal cortex, supramarginal gyrus, postcentral cortex and posterior insula, regions that play roles in cognitive, visuospatial, somatosensory and reward-processing functions and are commonly compromised in alcoholism. Indeed, low scores on psychomotor and episodic memory tests in alcoholics were significantly related to the aberrant orbitofrontal HF power.

BOLD signal oscillation power dynamics are frequency specific for both groups

Resting-state fMRI analyses typically focus on LF and MF spectra, usually below 0.08 Hz. Expanding this range to identify regional information of HF oscillation power revealed the frequency-dependent power spectrum organization and novel findings implicating physiological mechanisms for some alcoholism-related deficits. Comparing MF and LF bands, MF power was higher in subcortical regions and LF power higher in cortical regions, which was consistent with previous studies (Chen *et al.* 2015; Wang *et al.* 2016). Contrasting the HF with the LF bands enhanced the distinction of frequency power spectra between cortical and subcortical areas (shown between Fig. 1a and c). This observation supports the position that brain regions have their own distinctive power distribution properties. With converging evidence from two other studies (Wang *et al.* 2014; Xue *et al.* 2014), our results also suggest a specific functional role of the thalamus that is characterized by MF power. We infer that the MF specificity for the thalamus may reflect inherent thalamic neuronal rhythmicity (Steriade *et al.* 1993), supporting its role in relaying information from cortical and subcortical areas.

Although the link between the frequency-specific oscillation power distribution and physiological functions is not yet fully understood, studies have suggested that neuronal properties and cytoarchitectonic complexity may contribute to regional frequency characteristics of BOLD oscillation power. LF signals usually arise from neurons that serve long-distance connections in largerscale neural networks. Neurons with more complexity

confined in a smaller neuronal space usually involve HF BOLD oscillation (Buzsaki & Draguhn 2004; Baria *et al.* 2011; Chen *et al.* 2015; Wang *et al.* 2016). With these differences, exploration of these organized oscillation properties may identify abnormal neuronal activities and understand the pathophysiology of diseases.

Aberrant frequency oscillation power in alcoholism

Frequency oscillation power in alcoholics was different from that in controls in several cortical regions, most notably the orbitofrontal cortex. Previously, the LF power abnormality in orbitofrontal cortex has been observed in people with depressive disorder (Zhang *et al.* 2016) and antisocial personality disorder (Liu *et al.* 2014b). Yet our results showed that aberrant frequency power in orbitofrontal cortex occurred in particular within the HF bandwidth. This emphasizes the relevance of insult in alcoholism in regard to spontaneous intrinsic BOLD oscillations and their underlying neuronal activities of the orbitofrontal cortex.

The orbitofrontal cortex is structurally and functionally connected to subcortical reward-associated and arousal-associated regions including amygdala, hippocampus, ventral striatum and nucleus accumbens (Barbas 2007) and engages in sensory integration, reward processing, memory and reward-related decision making using subcortico-cortical connections (Kringelbach 2005; Goldstein & Volkow 2011; Wikenheiser & Schoenbaum 2016). Some fMRI studies have shown aberrations of orbitofrontal BOLD signals in alcoholics, who exhibited greater orbitofrontal cortex activation than controls in response to alcohol-related stimuli (Tapert *et al.* 2003), a pattern that correlated with higher subjective alcohol craving (Myrick *et al.* 2004), suggesting that hyperactivation of the orbitofrontal cortex can contribute to increased reward expectancy and addictive behaviors. Aberration in orbitofrontal neurofunctional dynamics in the HF band could affect inter-regional communication. For example, we recently showed that alcoholics had greater functional connectivity than controls between inferior prefrontal/orbitofrontal cortex (BA11/47) and anterior cingulate cortex (Müller-Oehring *et al.* 2014), a hub in the salience network, shaping the interaction of rewardassociated behaviors with incentive salience in alcoholics.

Notably, greater orbitofrontal HF power in alcoholics was associated with poorer verbal memory, logical memory and graphomotor abilities. Although the role of the orbitofrontal cortex is not directly associated with these abilities, HF power predominant regions such as hippocampus and striatum, which are functionally connected to the orbitofrontal cortex, do play important roles in memory, learning and motor function (Mattfeld & Stark 2015). Overall, the increased orbitofrontal oscillation power in the alcoholic brain might index a shift in its frequency power distribution and serve as a neural marker for a greater engagement of reward system nodes at the expense of perceptual-motor and memory processing efficiency.

Another brain region that plays an integrator role between subcortical limbic-striatal and cortical regions is the insular cortex. We observed aberrant frequency power of the posterior insula in the alcoholic brain in the HF band, which is sensitive in detecting subcortical regional oscillation power. The link between insula and alcoholism has been widely demonstrated: the insula has various roles in alcohol-related cue processing, reward-related

decision making, craving, conscious awareness and interoception (Garavan 2010; Naqvi *et al.* 2014). Further, the posterior insula, functionally connected to sensorimotor cortex, is responsible for relaying primary motor and sensory information to the sensorimotor cortex and the anterior insula (Cauda *et al.* 2011). Recently, Migliorini *et al.* (2013) demonstrated that people with substance use disorders including alcoholics had attenuated posterior insula activation in response to sensory stimulation. This finding is consistent with attenuated perfusion of the insula detected with arterial spin labeling in alcoholics (Sullivan *et al.* 2013). The observed diagnosis-specific difference in HF oscillation power of the posterior insula adds to previous results and emphasizes the functional role of this region in alcoholism. Altered frequency oscillation power in brain regions that link subcortico-cortical circuits may reflect aberrations in intrinsic neuronal rhythmicity (Steriade *et al.* 1993) and affect how information is converged from cortical and subcortical areas.

Group differences for MF and LF oscillation power were observed in posterior brain regions where alcoholics exhibited greater left postcentral and occipito-temporal ALFF power and less right parietal ALFF power than controls. Studying resting-state default mode network relative to active task-engaged networking in alcoholism, Chanraud *et al.* (2011) previously observed stronger connectivity between the posterior cingulate cortex and the postcentral cortex during a spatial working memory task in alcoholics relative to controls. Similarly, Krienke *et al.* (2014) found greater posterior cingulate cortex connectivity to postcentral and temporal regions in sober alcoholics than controls while viewing alcohol-related video sequences stimulating cue-induced cravings. Even during simple motor tasks, alcoholics were found to recruit additional postcentral and temporal regions in contrast to controls (Parks *et al.* 2010). Thus, alcoholics in these studies exhibited similar task-activated posterior regional activation patterns not seen in controls. In our study, however, spontaneous fluctuations of the BOLD response were observed during rest and not in response to a task. Accordingly, the identified group differences may essentially describe a shift in the regional BOLD frequency power spectrum in chronic alcoholics with potential consequences for abnormal inter-regional synchronization when tasks engage posterior brain networks, e.g., when comparing incoming visual stimuli with experiences (Krienke *et al.* 2014). Finally, we observed less LF oscillation power in the parietal cortex including the supramarginal gyrus in alcoholics than in controls. Compromise of parietal regions in alcoholism has been previously associated with impairments of working memory, visuospatial and attentional abilities (Stavro, Pelletier, & Potvin 2013). These findings lead to the speculation that BOLD frequency power dynamics depend on the relative role a region plays within cortico-cortical and subcortico-cortical networks and that the pattern of intrinsic regional frequency power aberration may be indicative of altered neurobiological mechanisms in alcoholism.

Gray matter volume deficits occur in chronic alcoholism (Grodin *et al.* 2013) and can be a confounding factor for rs-fMRI functional connectivity and taskevoked BOLD signal analysis. However, the frequency oscillation power analyses used in the current study is relatively insensitive to structural alterations with limited effect on frequency power results (Aiello *et al.* 2015; Liu *et al.* 2014a). Therefore, the main results found in the current study were unlikely due to structural differences in alcoholics compared with controls. One limitation was that one-third of the sample had incomplete neuropsychological datasets; yet

the sample size for the significant FDR-corrected correlation results was never fewer than 32 per group.

In summary, we demonstrated that the frequency power spectra detected with BOLD were systematically organized within the subcortical and cortical regions. This architecture likely reflects inherent neurophysiological properties (Buzsaki & Draguhn 2004) and therefore can provide novel insights about the frequency-specific aberrations of these regional oscillation power dynamics to explain alcoholism-related impairments of reward, visuomotor, memory and sensory processing. Our findings emphasize the value of taking the full frequency bandwidth into account to unveil the intrinsic pathophysiological mechanisms that may serve as potential biomarkers for identifying mechanisms of cognitive impairment in chronic alcoholism.

Acknowledgement

The authors declare no competing financial interests. This study is supported by National Institutes of Health grants AA023165, AA017168 and AA005965.

References

Aiello M, Salvatore E, Cachia A, Pappata S, Cavaliere C, Prinster A, Nicolai E, Salvatore M, Baron JC, Quarantelli M (2015) Relationship between simultaneously acquired resting-state regional cerebral glucose metabolism and functional MRI: a PET/MR hybrid scanner study. Neuroimage 113:111–121. [PubMed: 25791784]

Babor T, Higgins-Biddle JC, Saunders JB, Monteiro MG (2001) AUDIT—The Alcohol Use Disorders Identification Test: Guidelines for Use in Primary Care World Health Organizaton Department of Mental Health and Substance Abuse: Geneva.

Baliki MN, Baria AT, Apkarian AV (2011) The cortical rhythms of chronic back pain. J Neurosci 31:13981–13990. [PubMed: 21957259]

Barbas H (2007) Flow of information for emotions through temporal and orbitofrontal pathways. J Anat 211:237–249. [PubMed: 17635630]

Baria AT, Baliki MN, Parrish T, Apkarian AV (2011) Anatomical and functional assemblies of brain BOLD oscillations. J Neurosci 31:7910–7919. [PubMed: 21613505]

Baria AT, Mansour A, Huang L, Baliki MN, Cecchi GA, Mesulam MM, Apkarian AV (2013) Linking human brain local activity fluctuations to structural and functional network architectures. Neuroimage 73:144–155. [PubMed: 23396160]

Beck AT, Steer RA, Brown GK (1996) BDI-II, Beck Depression Inventory: Manual Psychological Corp: Harcourt Brace: San Antonio, Tex.; Boston.

Benjamini Y, Krieger AM, Yekutieli D (2006) Adaptive linear step-up procedures that control the false discovery rate. Biometrika 93:491–507.

Biswal B, Yetkin FZ, Haughton VM, Hyde JS (1995) Functional connectivity in the motor cortex of resting human brain using echo-planar MRI. Magn Reson Med 34:537–541. [PubMed: 8524021]

Buzsaki G, Draguhn A (2004) Neuronal oscillations in cortical networks. Science 304:1926–1929. [PubMed: 15218136]

Camchong J, Stenger A, Fein G (2013) Resting-state synchrony in long-term abstinent alcoholics. Alcohol Clin Exp Res 37:75–85. [PubMed: 22725701]

Cauda F, D'Agata F, Sacco K, Duca S, Geminiani G, Vercelli A (2011) Functional connectivity of the insula in the resting brain. Neuroimage 55:8–23. [PubMed: 21111053]

Chanraud S, Pitel AL, Pfefferbaum A, Sullivan EV (2011) Disruption of functional connectivity of the default-mode network in alcoholism. Cereb Cortex 21:2272–2281. [PubMed: 21368086]

Chen YC, Xia W, Luo B, Muthaiah VP, Xiong Z, Zhang J, Wang J, Salvi R, Teng GJ (2015) Frequency-specific alternations in the amplitude of low-frequency fluctuations in chronic tinnitus. Front Neural Circuits 9:67. [PubMed: 26578894]

Courtney KE, Ghahremani DG, Ray LA (2013) Fronto-striatal functional connectivity during response inhibition in alcohol dependence. Addict Biol 18:593–604. [PubMed: 23240858]

Delis DC, Kramer J, Kaplan E, Ober BA (2000) CVLT-II: California Verbal Learning Test: Adult Version Psychological Corporation.

Esposito F, Tessitore A, Giordano A, De Micco R, Paccone A, Conforti R, Pignataro G, Annunziato L, Tedeschi G (2013) Rhythm-specific modulation of the sensorimotor network in drug-naive patients with Parkinson's disease by levodopa. Brain 136:710–725. [PubMed: 23423673]

Fair DA, Nigg JT, Iyer S, Bathula D, Mills KL, Dosenbach NU, Schlaggar BL, Mennes M, Gutman D, Bangaru S, Buitelaar JK, Dickstein DP, Di Martino A, Kennedy DN, Kelly C, Luna B, Schweitzer JB, Velanova K, Wang YF, Mostofsky S, Castellanos FX, Milham MP (2012) Distinct neural signatures detected for ADHD subtypes after controlling for micromovements in resting state functional connectivity MRI data. Front Syst Neurosci 6:80. [PubMed: 23382713]

First MB, Spitzer RL, Gibbon M, Williams JBW (2012) Structured Clinical Interview for DSM-IV® Axis I Disorders (SCID-I), Clinician Version American Psychiatric Publishing: Administration Booklet.

Garavan H (2010) Insula and drug cravings. Brain Struct Funct 214:593–601. [PubMed: 20512373]

Goldstein RZ, Volkow ND (2011) Dysfunction of the prefrontal cortex in addiction: neuroimaging findings and clinical implications. Nat Rev Neurosci 12:652–669. [PubMed: 22011681]

Grodin EN, Lin H, Durkee CA, Hommer DW, Momenan R (2013) Deficits in cortical, diencephalic and midbrain gray matter in alcoholism measured by VBM: effects of co-morbid substance abuse. Neuroimage Clin 2:469–476. [PubMed: 24179800]

Kong XZ, Zhen Z, Li X, Lu HH, Wang R, Liu L, He Y, Zang Y, Liu J (2014) Individual differences in impulsivity predict head motion during magnetic resonance imaging. PLoS One 9: e104989. [PubMed: 25148416]

Krienke UJ, Nikesch F, Spiegelhalder K, Hennig J, Olbrich HM, Langosch JM (2014) Impact of alcohol-related video sequences on functional MRI in abstinent alcoholics. Eur Addict Res 20:33–40. [PubMed: 23921439]

Kringelbach ML (2005) The human orbitofrontal cortex: linking reward to hedonic experience. Nat Rev Neurosci 6:691–702. [PubMed: 16136173]

Le Berre AP, Sullivan EV (2016) Anosognosia for memory impairment in addiction: insights from neuroimaging and neuropsychological assessment of metamemory. Neuropsychol Rev

Liu C, Li C, Yin X, Yang J, Zhou D, Gui L, Wang J (2014a) Abnormal intrinsic brain activity patterns in patients with subcortical ischemic vascular dementia. PLoS One 9: e87880. [PubMed: 24498389]

Liu H, Liao J, Jiang W, Wang W (2014b) Changes in lowfrequency fluctuations in patients with antisocial personality disorder revealed by resting-state functional MRI. PLoS One 9: e89790. [PubMed: 24598769]

Loeber S, Vollstadt-Klein S, von der Goltz C, Flor H, Mann K, Kiefer F (2009) Attentional bias in alcohol-dependent patients: the role of chronicity and executive functioning. Addict Biol 14:194–203. [PubMed: 19291010]

Malinen S, Vartiainen N, Hlushchuk Y, Koskinen M, Ramkumar P, Forss N, Kalso E, Hari R (2010) Aberrant temporal and spatial brain activity during rest in patients with chronic pain. Proc Natl Acad Sci U S A 107:6493–6497. [PubMed: 20308545]

Mattfeld AT, Stark CEL (2015) Functional contributions and interactions between the human hippocampus and subregions of the striatum during arbitrary associative learning and memory. Hippocampus 25:900–911. [PubMed: 25560298]

Migliorini R, Stewart JL, May AC, Tapert SF, Paulus MP (2013) What do you feel? Adolescent drug and alcohol users show altered brain response to pleasant interoceptive stimuli. Drug Alcohol Depend 133:661–668. [PubMed: 24071571]

Müller-Oehring EM, Schulte T (2014) Cognition, emotion, and attention. Handb Clin Neurol 125:341–354. [PubMed: 25307584]

Müller-Oehring EM, Jung YC, Pfefferbaum A, Sullivan EV, Schulte T (2014) The resting brain of alcoholics. Cereb Cortex

Myrick H, Anton RF, Li X, Henderson S, Drobes D, Voronin K, George MS (2004) Differential brain activity in alcoholics and social drinkers to alcohol cues: relationship to craving. Neuropsychopharmacology 29:393–402. [PubMed: 14679386]

Naqvi NH, Gaznick N, Tranel D, Bechara A (2014) The insula: a critical neural substrate for craving and drug seeking under conflict and risk. Ann N Y Acad Sci 1316:53–70. [PubMed: 24690001]

Padula CB, Anthenelli RM, Eliassen JC, Nelson E, Lisdahl KM (2015) Gender effects in alcohol dependence: an FMRI pilot study examining affective processing. Alcohol Clin Exp Res 39:272–281. [PubMed: 25684049]

Parks MH, Greenberg DS, Nickel MK, Dietrich MS, Rogers BP, Martin PR (2010) Recruitment of additional brain regions to accomplish simple motor tasks in chronic alcohol-dependent patients. Alcohol Clin Exp Res 34:1098–1109. [PubMed: 20374203]

Power JD, Barnes KA, Snyder AZ, Schlaggar BL, Petersen SE (2012) Spurious but systematic correlations in functional connectivity MRI networks arise from subject motion. Neuroimage 59:2142–2154. [PubMed: 22019881]

Power JD, Schlaggar BL, Petersen SE (2015) Recent progress and outstanding issues in motion correction in resting state fMRI. Neuroimage 105:536–551. [PubMed: 25462692]

Stavro K, Pelletier J, Potvin S (2013) Widespread and sustained cognitive deficits in alcoholism: a meta-analysis. Addict Biol 18:203–213. [PubMed: 22264351]

Steriade M, Contreras D, Curro Dossi R, Nunez A (1993) The slow (<1 Hz) oscillation in reticular thalamic and thalamocortical neurons: scenario of sleep rhythm generation in interacting thalamic and neocortical networks. J Neurosci 13:3284–3299. [PubMed: 8340808]

Sullivan EV, Müller-Oehring E, Pitel AL, Chanraud S, Shankaranarayanan A, Alsop DC, Rohlfing T, Pfefferbaum A (2013) A selective insular perfusion deficit contributes to compromised salience network connectivity in recovering alcoholic men. Biol Psychiatry 74:547–555. [PubMed: 23587427]

Tapert SF, Cheung EH, Brown GG, Frank LR, Paulus MP, Schweinsburg AD, Meloy MJ, Brown SA (2003) Neural response to alcohol stimuli in adolescents with alcohol use disorder. Arch Gen Psychiatry 60:727–735. [PubMed: 12860777]

Wang Z, Zhang Z, Liao W, Xu Q, Zhang J, Lu W, Jiao Q, Chen G, Feng J, Lu G (2014) Frequency-dependent amplitude alterations of resting-state spontaneous fluctuations in idiopathic generalized epilepsy. Epilepsy Res 108:853–860. [PubMed: 24721198]

Wang L, Kong Q, Li K, Su Y, Zeng Y, Zhang Q, Dai W, Xia M, Wang G, Jin Z, Yu X, Si T (2016) Frequency-dependent changes in amplitude of low-frequency oscillations in depression: a resting-state fMRI study. Neurosci Lett 614:105–111. [PubMed: 26797652]

Wechsler D (1981) WAIS-R Manual: Wechsler Adult Intelligence Scale-Revised Psychological Corporation New York.

Wechsler D (2001) Wechsler Test of Adult Reading: WTAR San Antonio, Tex: Psychological Corp.

Wechsler D, Stone CP (1987) Wechsler Memory Scale-Revised Psychological Corporation.

Weiland BJ, Welsh RC, Yau WY, Zucker RA, Zubieta JK, Heitzeg MM (2013) Accumbens functional connectivity during reward mediates sensation-seeking and alcohol use in highrisk youth. Drug Alcohol Depend 128:130–139. [PubMed: 22958950]

Wikenheiser AM, Schoenbaum G (2016) Over the river, through the woods: cognitive maps in the hippocampus and orbitofrontal cortex. Nat Rev Neurosci 17:513–523. [PubMed: 27256552]

Xue SW, Li D, Weng XC, Northoff G, Li DW (2014) Different neural manifestations of two slow frequency bands in resting functional magnetic resonance imaging: a systemic survey at regional, interregional, and network levels. Brain Connect 4:242–255. [PubMed: 24456196]

Yan CG, Cheung B, Kelly C, Colcombe S, Craddock RC, Di Martino A, Li Q, Zuo XN, Castellanos FX, Milham MP (2013) A comprehensive assessment of regional variation in the impact of head micromovements on functional connectomics. Neuroimage 76:183–201. [PubMed: 23499792]

Yan CG, Wang XD, Zuo XN, Zang YF (2016) DPABI: Data Processing & Analysis for (Resting-State) Brain Imaging. Neuroinformatics

Yang Y, Zhong N, Imamura K, Lu S, Li M, Zhou H, Li H, Yang X, Wan Z, Wang G, Hu B, Li K (2016) Task and resting-state fMRI reveal altered salience responses to positive stimuli in patients with major depressive disorder. PLoS One 11: e0155092. [PubMed: 27192082]

Zang YF, He Y, Zhu CZ, Cao QJ, Sui MQ, Liang M, Tian LX, Jiang TZ, Wang YF (2007) Altered baseline brain activity in children with ADHD revealed by resting-state functional MRI. Brain Dev 29:83–91. [PubMed: 16919409]

Zhang J, Wei L, Hu X, Zhang Y, Zhou D, Li C, Wang X, Feng H, Yin X, Xie B, Wang J (2013) Specific frequency band of amplitude low-frequency fluctuation predicts Parkinson's disease. Behav Brain Res 252:18–23. [PubMed: 23727173]

Zhang X, Di X, Lei H, Yang J, Xiao J, Wang X, Yao S, Rao H (2016) Imbalanced spontaneous brain activity in orbitofrontal-insular circuits in individuals with cognitive vulnerability to depression. J Affect Disord 198:56–63. [PubMed: 27011360]

Zheng H, Kong L, Chen L, Zhang H, Zheng W (2015) Acute effects of alcohol on the human brain: a resting-state FMRI study. Biomed Res Int 2015: 947529. [PubMed: 25705701]

Zuo XN, Di Martino A, Kelly C, Shehzad ZE, Gee DG, Klein DF, Castellanos FX, Biswal BB, Milham MP (2010) The oscillating brain: complex and reliable. Neuroimage 49: 1432–1445. [PubMed: 19782143]

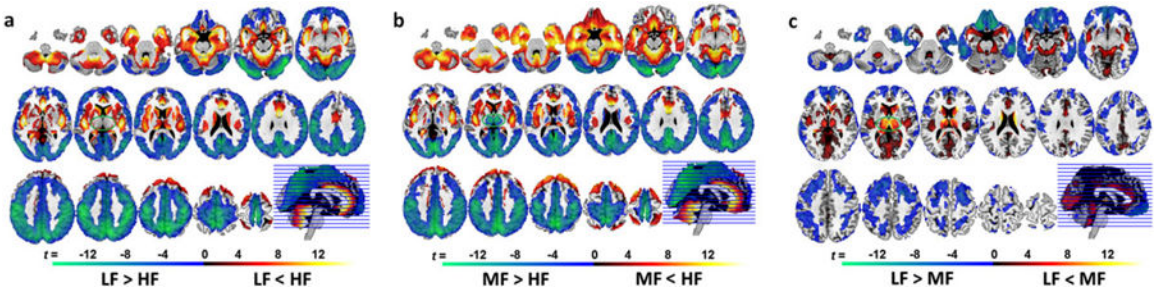

Figure 1.

Whole-brain spatial frequency power distribution. Frequency-specific power spectra maps across all subjects for (a) low-frequency (LF) band versus high-frequency (HF) band; (b) middle-frequency (MF) band versus HF band; (c) LF band versus MF band. The frequency power differences depicted here reflect regional physiological properties and regional specificity to certain frequency bands. The rainbow color bar indicates relative ALFF values. The green–blue–red–yellow color bar represents *t*-scores ≥ 2.81 (P_{peak} = 0.005, two-tailed) indicative of significant frequency power differences in the paired comparisons between the three frequency bands

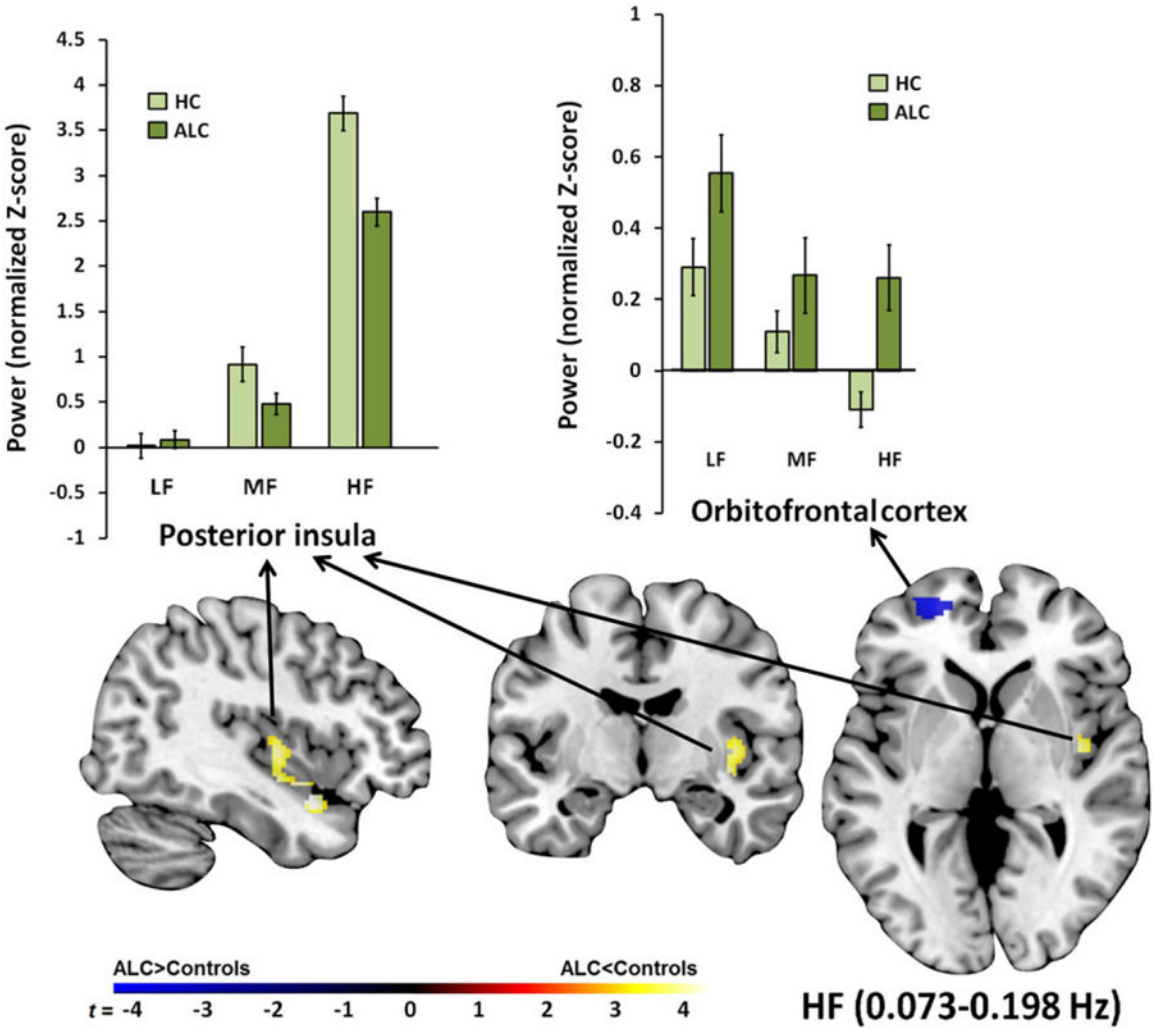

Figure 2.

Regional high-frequency (HF) power differences between alcoholics and controls. The alcoholics (ALC) had greater HF power in the orbitofrontal cortex compared with controls. Although HF was the dominant frequency power spectrum in the posterior insula for controls and ALC, ALC exhibited less HF power in this region than controls. The color bar indicates *t*-scores for group differences of frequency power. The bar graphs show normalized Z-scores for ALFF power extracted from each significant cluster for each group and frequency band. LF, low frequency; MF, middle frequency

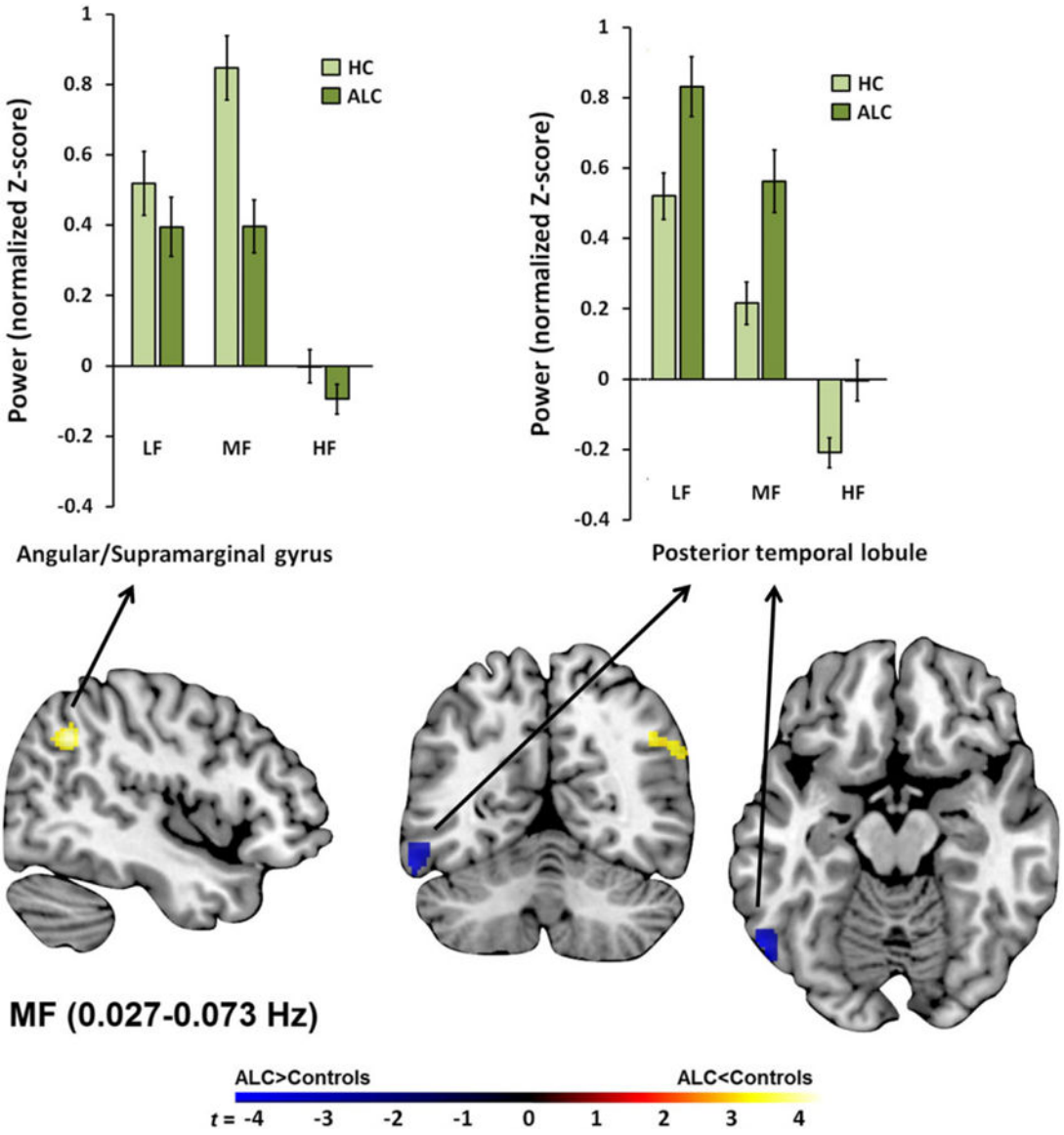

Figure 3.

Regional middle-frequency (MF) power differences between alcoholics (ALC) and controls. Depicted are significant group differences showing greater MF power in the postcentral and posterior temporal cortices and less MF power in the angular/supramarginal gyrus in ALC relative to controls. HF, high frequency; LF, low frequency

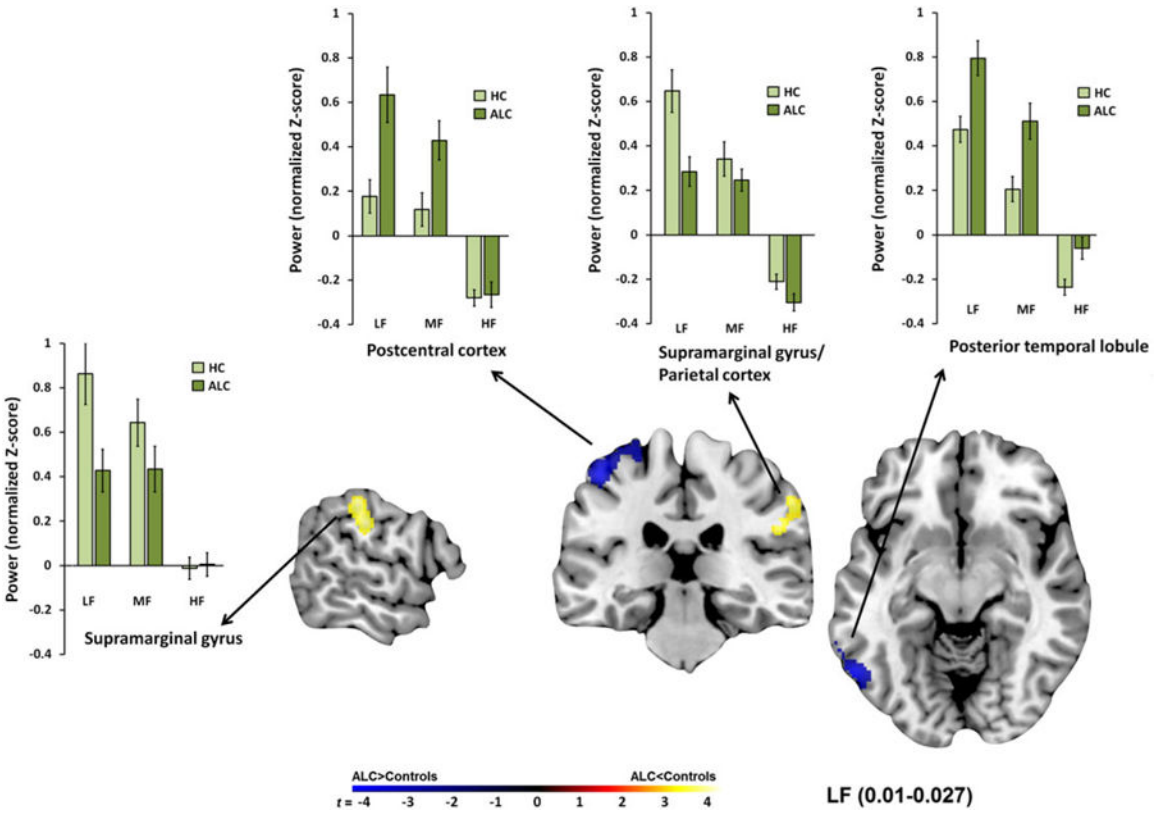

Figure 4.

Regional low-frequency (LF) power differences between alcoholics (ALC) and controls. The cortical regions were dominated by LF power in controls and ALC. Depicted here are significant group differences showing that ALC relative to controls had greater LF power in the postcentral and posterior temporal cortices and had lower LF power in the parietal cortex. HF, high frequency; MF, middle frequency

Table 1

Subject clinical and behavioral characteristics.

	C		*ALC*		*P*
	n	***Mean ± SD***	**n**	***Mean ± SD***	
M/W	39/17		39/17		1[a]
Age (years)	56	51.7 ± 10.32	56	51.15 ± 10.27	0.778
Education (years)	54	15.57 ± 2.41	56	13.2 ± 2.51	<0.001
SES	54	26.96 ± 11.87	56	42.3 ± 15.63	<0.001
Handedness (L/R/A)	2/49/5		3/51/2		0.47[a]
Lifetime alcohol consumption (kg)	56	45.5 ± 71.75	56	1173.54 ± 1004.67	<0.001
Days since last drink	54	861.98 ± 3251.1	56	276.21 ± 719.55	<0.001
Days since last met diagnosis criteria	—	—	56	75.58 ± 144.34	—
AUDIT	54	2.56 ± 2.61	51	17.55 ± 11.94	<0.001
Depressive symptoms score (BDI−II)	53	2.02 ± 2.93	56	8.82 ± 6.68	<0.001
Premorbid IQ (WTAR−SS)	48	110.4 ± 14.4	49	96.84 ± 19.42	<0.001
Logical memory I (WMS−R)	37	25.78 ± 7.22	41	18.68 ± 8.89	<0.001
Logical memory II (WMS−R)	37	22.22 ± 7.33	41	15.2 ± 8.7	<0.001
Total free recall (CVLT−II)	33	50.46 ± 9.08	35	41.83 ± 12.66	0.002
Delayed free recall (CVLT−II)	33	11.3 ± 2.63	35	8.69 ± 3.8	0.002
Graphomotor speed (WAIS−R)	32	56.94 ± 11.97	33	44.67 ± 13.61	<0.001
Time to complete DS (seconds) (WAIS−R)	32	151.59 ± 34.33	33	191.21 ± 53.47	0.001
Scanner (3T Signa/MR750)	26/30		25/31		0.85[a]

A = ambidextrous; ALC = alcoholics; AUDIT = alcohol use disorders identification test; BDI−II = Beck Depression Inventory; C = controls; CVLT− II = California Verbal Learning Test−II; DS = Digit Symbol subtest; L = left; Logical memory I of the Wechsler Memory Scale−Revised = immediate recall; Logical memory II of the Wechsler Memory Scale−Revised = delayed recall; M = men; *S* = number; R = right; SD = standard deviation; SES = socioeconomic status: higher scores represent lower SES (range, 11–77); W = women; WAIS−R = Wechsler Adult Intelligence Scale−Revised; WMS−R = Wechsler Memory Scale−Revised; WTAR−SS = standard score of the Wechsler Test of Adult Reading.

[a] χ^2 test; statistical significance level was set at $P < 0.05$.

Table 2

Significant group differences in ALFF values within frequency bands.

Regions		*H*	*k*	*MNI coordinates*			*t− score*	*Z−score*
				x	*y*	*z*		
HF (0.073–0.198 Hz)								
C > ALC	Posterior insula[a]	R	182	42	8	−20	4.56	4.48
				40	−6	2	3.72	3.68
				38	−6	−6	3.64	3.6
ALC > C	Orbitofrontal cortex (BA10/11/47)	L	126	−26	54	0	3.77	3.73
MF (0.027–0.073 Hz)								
C > ALC	Angular/supramarginal gyrus	R	131	44	−56	36	4.03	3.98
				56	−60	30	3.14	3.11
				50	−64	36	2.95	2.93
ALC > C	Posterior inferior/middle temporal lobule[a]	L	128	−58	−64	−14	4.65	4.57
LF (0.01–0.027 Hz)								
C > ALC	Supramarginal gyrus[a]	R	254	52	−26	26	3.84	3.79
				62	−22	32	3.63	3.59
				60	−26	40	3.6	3.57
	Supramarginal gyrus/inferior/superior	R	161	42	−42	62	4.33	4.27
	Parietal cortex			28	−38	44	3.82	3.77
ALC > C	Postcentral cortex[a]	L	285	−46	−28	56	4.69	4.61
				−26	−30	66	3.43	3.4
	Posterior inferior/middle temporal lobule[a]	L	153	−58	−62	−10	4.91	4.82
				−68	−48	−8	3.75	3.71

ALC = alcoholics; ALFF = amplitude of low frequency fluctuation; BA = Brodmann area; C = controls; H = hemisphere; *k* = number of brain voxels in a cluster; L = left; MNI = Montreal Neurological Institute coordinates (*x*, *y* and *z*) for peak voxels within a significant cluster; R = right. Note: Results were confirmed with reslicing into 3 × 3 × 3 voxel space.

[a]For $t = 3.38$, $P_{peak} = 0.001$, two−tailed, cluster−corrected for multiple comparisons at $P_{corrected} < 0.05$.